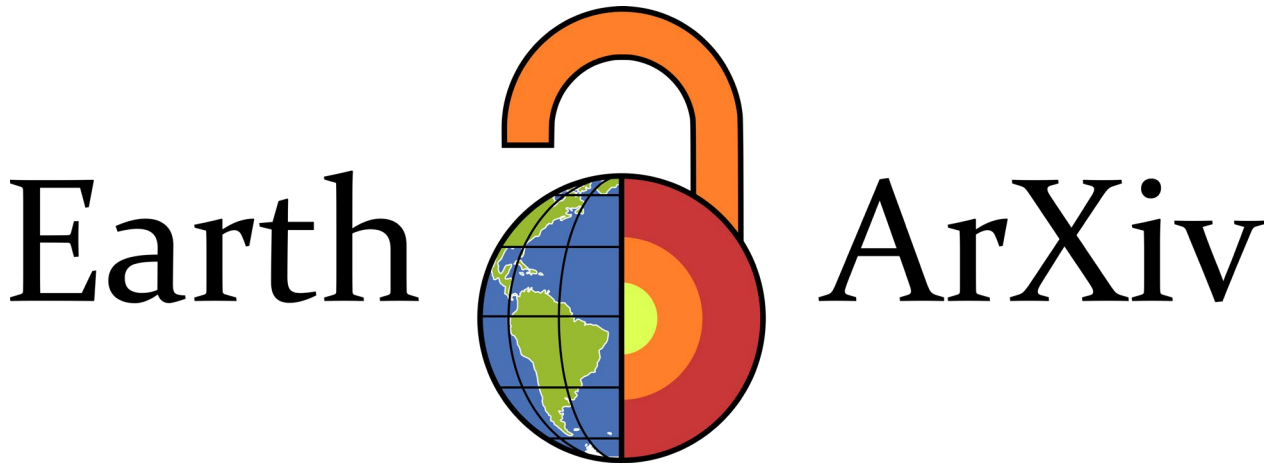

Long-term future Greenland ice loss determined by peak global warming

Matteo Willeit[1*], Alexander Robinson[2], Christine Kaufhold[1,3] and Andrey Ganopolski[1]

[1]Earth System Analysis, Potsdam Institute for Climate Impact Research (PIK), Member of the Leibniz Association, Potsdam, Germany.
[2]Earth System Complexity, Alfred Wegener Institute, Helmholtz Centre for Polar and Marine Research, Potsdam, Germany.
[3]Institute of Physics and Astronomy, Universität Potsdam, Potsdam, Germany.

*Corresponding author(s). E-mail(s): willeit@pik-potsdam.de;

This manuscript has been submitted for publication in Nature Climate Change. Please note the manuscript has yet to be formally accepted for publication. Subsequent versions of this manuscript may have slightly different content. If accepted, the final version of this manuscript will be available via the 'Peer-reviewed Publication DOI' link on the right-hand side of this webpage. Please feel free to contact any of the authors; we welcome feedback.

Long-term future Greenland ice loss determined by peak global warming

Matteo Willeit[1*], Alexander Robinson[2], Christine Kaufhold[1,3], Andrey Ganopolski[1]

[1]Earth System Analysis, Potsdam Institute for Climate Impact Research (PIK), Member of the Leibniz Association, Potsdam, Germany.
[2]Earth System Complexity, Alfred Wegener Institute, Helmholtz Centre for Polar and Marine Research, Potsdam, Germany.
[3]Institute of Physics and Astronomy, Universität Potsdam, Potsdam, Germany.

*Corresponding author(s). E-mail(s): willeit@pik-potsdam.de;
Contributing authors: alexander.robinson@awi.de;
kaufhold@pik-potsdam.de; andrey@pik-potsdam.de;

Abstract

The Greenland ice sheet (GrIS) is known to be very sensitive to climate change, and persistent global warming only slightly higher than today could be enough to completely melt it. However, the implications of a temporary crossing of this temperature threshold for future GrIS mass loss remain unknown. Here we present simulations of the next 10,000 years under different future anthropogenic emissions scenarios, performed using a fully coupled Earth system model. We find that long-term Greenland ice loss is determined by the peak global temperature increase, which generally occurs within the next few centuries. The GrIS contribution to sea-level rise after 10,000 years increases by ∼1.5 m for each degree of warming above a critical peak global warming threshold of ∼1.5°C, which is close to the GrIS equilibrium tipping point. This finding is robust for different equilibrium climate sensitivities and across different scenarios. We also find that accounting for changes in the Earth's orbital parameters over the next 10,000 years substantially increases the sensitivity of the GrIS mass loss to anthropogenic warming. Our results demonstrate how 21st century climate policy will largely determine the fate of the GrIS for millennia to come.

Keywords: Greenland ice sheet, Future projections, Sea level, Tipping points

1 Introduction

The Greenland Ice Sheet (GrIS) is the second-largest body of ice on Earth, holding an ice volume of ∼7 metres of sea-level equivalent [1]. Over recent decades, observational data and climate models have provided increasing evidence of its vulnerability to anthropogenic climate change, raising concerns about its long-term stability and its contribution to future sea-level rise [2]. Recent studies indicate that the GrIS has been experiencing accelerated mass loss over the past decades, primarily driven by increasing surface melt and enhanced ice discharge from outlet glaciers [3–8], and this trend is projected to continue into the future [9–12].

Most modelling studies of the GrIS response to global warming are limited to either the current century or the next few centuries [13–17], with the results of these studies reviewed in IPCC assessment reports [2]. However, due to the inertia of the GrIS and the long atmospheric lifetime of anthropogenic CO_2 [18–20], the GrIS will continue to evolve for a very long time, even after the complete cessation of anthropogenic emissions. Fewer studies have been devoted to the stability of the GrIS and its long-term (millennial to multi-millennial) response to global warming. These studies generally indicate that if warming exceeds a critical threshold, the GrIS could contribute several metres to global sea-level rise over the coming centuries to millennia [21–28]. Model simulations also show that a partial or complete melting of the GrIS would represent an effectively irreversible commitment to multi-metre sea-level rise [23, 29, 30].

Idealised modelling studies indicate the presence of a tipping point for the GrIS, with sustained global warming above ∼1–3°C relative to pre-industrial conditions leading to complete melt of the ice sheet [23, 27, 31–35] due to strong positive feedbacks, namely the ice–elevation and the ice–albedo feedbacks. The existence of this tipping point is supported by palaeoclimate evidence suggesting that sustained temperatures ∼2°C above pre-industrial levels could lead to significant ice-sheet retreat [36–38].

Here we use a fast Earth system model with a coupled GrIS and interactive atmospheric CO_2 and CH_4 concentrations to explore the evolution of the GrIS over the next 10,000 years with emission levels compatible with future policy-relevant scenarios. Our results emphasise how the long-term GrIS mass loss is related to the short-term climate warming, and connect the transient response with the equilibrium response of the ice sheet.

2 Results

2.1 Long-term future Greenland ice-sheet evolution

Due to the very long atmospheric lifetime of anthropogenic CO_2 [18–20], the long-term climate evolution over the next 10,000 years is largely determined by the anthropogenic carbon emissions over the next few centuries. Here we force the fully-coupled climate–carbon cycle–GrIS fast Earth system model CLIMBER-X [41–44] with different Shared Socioeconomic Pathways (SSP) scenarios [45] extended for 10,000 years into the future (Methods, Extended Data Fig. 1) and investigate the Earth-system response, with a focus on the evolution of the GrIS. As changes in the orbital configuration of the Earth are important on multi-millennial time scales, they are explicitly

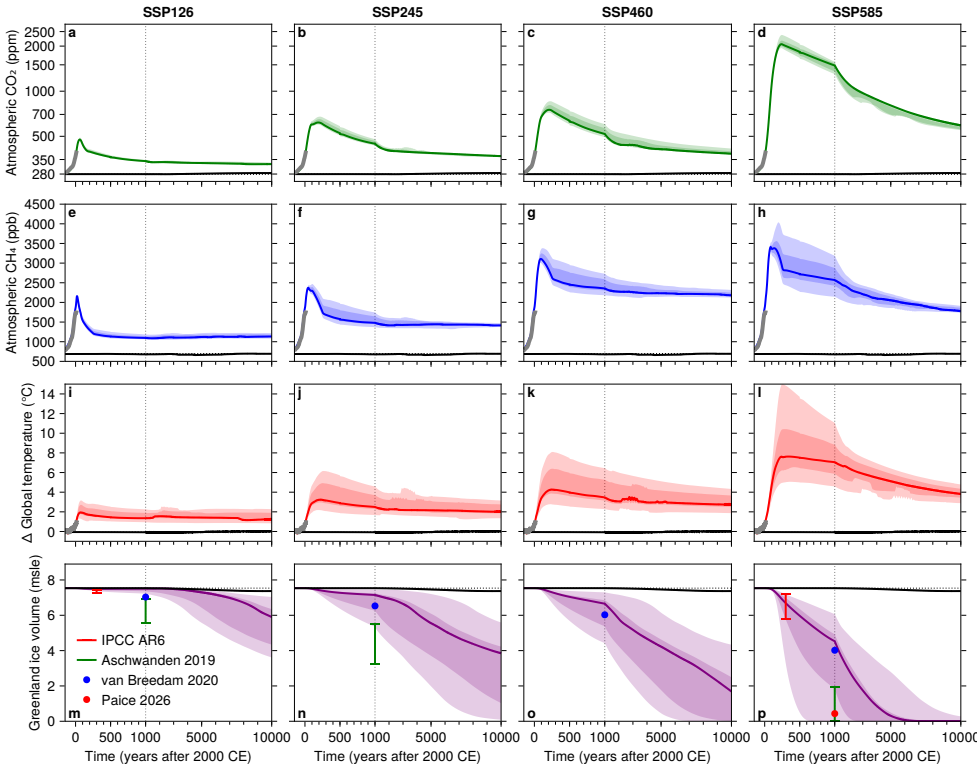

Fig. 1 Future climate and GrIS evolution. Simulated (**a**–**d**) atmospheric CO_2 and (**e**–**h**) CH_4 concentrations, (**i**–**l**) global temperature changes relative to pre-industrial conditions and (**m**–**p**) GrIS ice volume in metres sea-level equivalent (msle) in fully coupled climate–carbon cycle–GrIS model simulations of the next 10,000 years under four selected SSP scenarios. The coloured solid lines indicate the reference simulations with an ECS of ∼3°C; the dark shaded area represents the interquantile range and the light shaded area shows the full ensemble spread due to different ECS. The black solid lines indicate the simulated evolution under natural conditions (i.e. without anthropogenic forcing but with orbital forcing) and the dotted black lines represent a control simulation with constant pre-industrial conditions. The thick grey lines show the observed historical evolution of CO_2 (ref. [39]), CH_4 (ref. [39]) and global temperature (ref. [40]). In panels **m-p** the simulated GrIS melt is compared to previous studies as indicated by the legend in panel **m**. Simulations that produce a peak global warming of more than ∼15°C (i.e. simulations under SSP585 forcing with ECS larger than ∼4°C) are excluded from the figure.

considered in our experiments (Extended Data Fig. 1a-c). We account for uncertainties in future climate response by running an ensemble of model simulations where the radiative forcing of CO_2 is scaled to effectively represent different equilibrium climate sensitivities (ECS) in the 'very likely' IPCC range of 2–5°C (see ref. [46] and Methods for further details, and Supplementary Fig. S1 for a validation of the method). We additionally investigate the sensitivity of our results to key ice-sheet surface mass balance parameters (bare ice albedo and temperature lapse rate) and ice-sheet model parameters (flow enhancement factor and reference basal friction; see Methods). The

model performs well for the historical period (Supplementary Fig. S2), simulates a realistic GrIS at present (Extended Data Fig. 2), and shows a sensitivity of the GrIS surface mass balance to temperature changes that is consistent with estimates from regional climate models (Extended Data Fig. 3).

In the simulations, the peak concentrations of atmospheric CO_2 and CH_4 are generally reached in the next few centuries (Fig. 1a-h, Supplementary Fig. S3), with a subsequent decrease following a gradual reduction of anthropogenic emissions (Extended Data Fig. 1d,e) and continued net uptake of carbon by ocean and land. The global temperature evolution largely follows the radiative forcing of these GHGs, with an initial peak followed by a slow cooling trend (Fig. 1i-l). Different climate sensitivities result in a wide spread of possible temperature evolutions for a given SSP forcing scenario (Fig. 1i-l), with the range being further amplified by positive carbon-cycle feedbacks [46]. The surface mass balance of the GrIS rapidly decreases as the climate warms, but it remains positive for low emission scenarios. In high emission scenarios, surface mass balance can become negative depending on ECS (Supplementary Fig. S4g-i).

The GrIS evolution over the next 10,000 years strongly depends on the considered emissions scenario, with negligible or little ice loss in low emissions scenarios (e.g. SSP126), very uncertain ice loss in intermediate emission scenarios (e.g. SSP245 and SSP460) and complete loss of the GrIS in high emission scenarios (e.g. SSP585) (Fig. 1m-p). The large spread in possible GrIS evolutions under intermediate scenarios originates from the different ECS leading to very different global and regional climate warming. This is particularly relevant considering that, at present, intermediate scenarios represent the most likely future pathways [47]. The simulated GrIS mass loss in the next few centuries for different SSP scenarios is generally consistent with modelling studies summarised by the latest IPCC report [2], showing up to ∼1 msle of ice melt by the year 2300 in the SSP585 scenario (Fig. 1p). The few studies that extended the projections until the end of millennium show a relatively large spread of possible GrIS melt (Fig. 1m-p), with results from ref. [26] generally in line with those shown in this study, while ref. [24] shows a substantially higher sensitivity of the GrIS to warming. Under high emission scenarios, the GrIS completely melts within ∼5000 years in the reference runs, but as rapidly as ∼500 years if ECS is high (Fig. 1p). This is consistent with recent results from a coupled regional climate - ice sheet model showing an almost complete GrIS melt by the year 3000 CE under SSP585 [28] (Fig. 1p), when forced with large-scale climate change from a model with an ECS of almost 5°C.

2.2 Peak global warming crucial for fate of Greenland

The long-term GrIS volume loss can be approximately predicted from the peak global temperature rise across the ensemble of experiments with different scenarios and ECS (Fig. 2a). For peak warming below a critical value of ∼1.5°C (i.e. $\Delta T_{\mathrm{peak}}^{\mathrm{crit}}$) the committed sea-level rise from GrIS melt in 10,000 years is limited to less than 0.5 msle (Fig. 2a). For peak warming above this critical threshold, ice loss in 10,000 years rapidly increases with temperature, with a simulated sea-level rise from GrIS mass loss of ∼1.5 m for each additional °C of peak warming (Fig. 2a). For a peak global warming of more than ∼5°C, the GrIS melts completely in 10,000 years (Fig. 2a). In

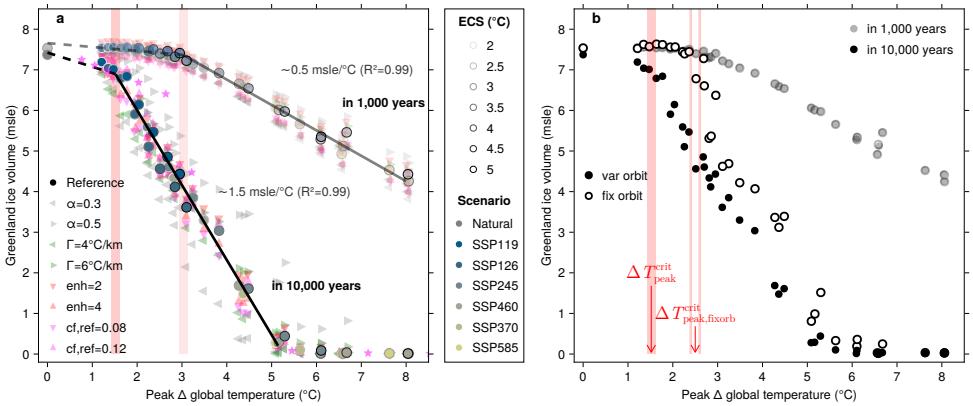

Fig. 2 Long-term Greenland ice loss as a function of peak global warming. **a** Simulated GrIS volume in metres of sea-level equivalent in 1,000 years and in 10,000 years (relative to 2000 CE) as a function of peak global warming relative to pre-industrial for all reference model simulations with different extended SSP scenarios (colours) and with different ECS (grey-scale shading of symbol outline). The best (in a RMSE sense) piecewise linear fits with automatic breakpoint detection are shown by the dashed and solid lines, with the shaded red vertical lines indicating the breakpoints for the 1,000 and 10,000 years time horizon. Simulations of the perturbed parameter ensemble are shown as well as semi-transparent markers, according to the legend in the lower-left corner. The magenta stars are estimates from idealised CO_2 emission simulations from ref. [25]. **b** Similar to **a** but additionally showing results from simulations with prescribed present-day orbital parameters (empty circles). The critical temperature thresholds for increased sensitivity of GrIS mass loss in 10,000 years to peak temperature for the cases with orbital forcing ($\Delta T^{\mathrm{crit}}_{\mathrm{peak}}$) and with fixed present-day orbit ($\Delta T^{\mathrm{crit}}_{\mathrm{peak,fixorb}}$) are identified at ∼1.5°C and ∼2.5°C, respectively, corresponding to the breakpoints in the piecewise linear fit, reflecting the inflection point in the scatterplot towards higher mass losses.

1,000 years, the contribution of the GrIS to sea-level rise is substantially lower, with ∼0.5 m for each °C of warming above ∼ 3°C (Fig. 2a). The results of the perturbed parameter ensemble confirm that the tight relation between long-term Greenland ice loss and peak global warming is robust (Fig. 2a), while the value of the $\Delta T^{\mathrm{crit}}_{\mathrm{peak}}$ and the slope of the linear fit shows a weak dependency to model parameters, with a generally higher sensitivity to surface mass balance parameters compared to ice-sheet parameters (Extended Data Fig. 4).

Given the tight relationship between GrIS volume and peak global warming in our simulations, it is possible to approximately determine the state of the GrIS for different levels of peak future global temperature rise and for different time horizons (Fig. 3). The GrIS generally starts to retreat from the south and from the north-west, while the ice over the western mountain ranges is the most resilient part of the GrIS (Fig. 3).

2.3 The impact of orbital forcing

While so far we have focused on the relation between Greenland mass loss and global warming, it is clear that summer temperature over Greenland is more relevant for the surface mass balance of the ice sheet as it controls the duration and intensity of the melt season.

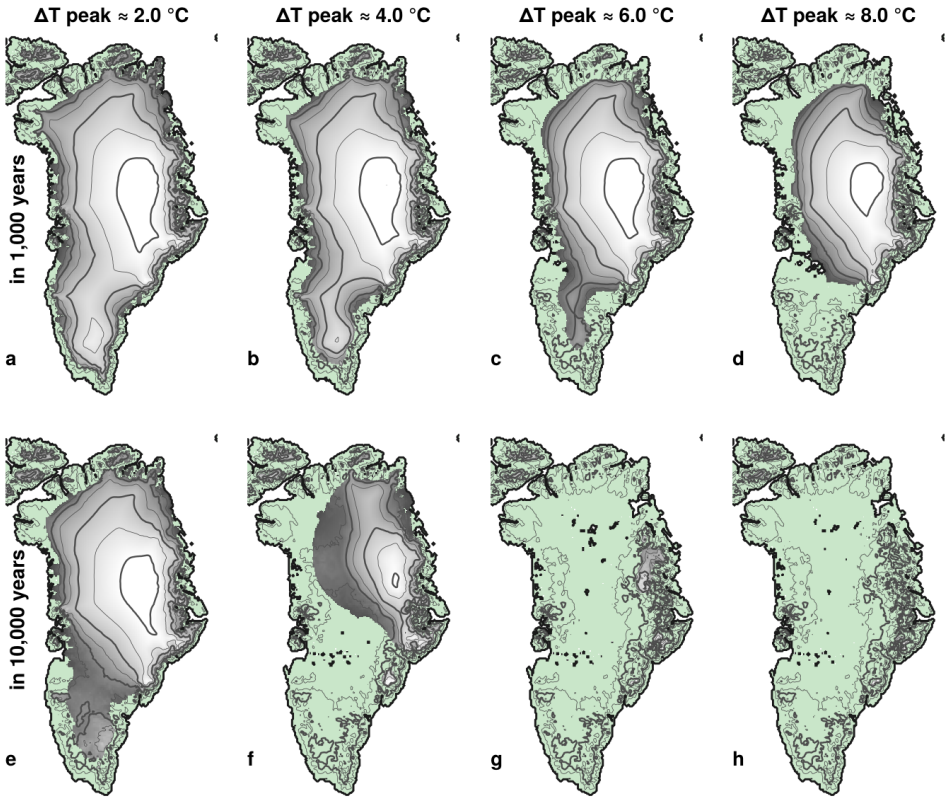

Fig. 3 GrIS for different levels of peak global warming. The simulated GrIS in 1,000 years (top) and in 10,000 years (bottom) for different levels of peak global warming of around 2, 4, 6 and 8°C, computed as an average over all different reference model simulations shown in Fig. 2a that fall within ±0.5°C of the respective peak warming. The elevation contour lines are spaced by 500 m, with the thick contour lines representing the 0, 1000, 2000 and 3000 m elevation isolines.

Due to polar amplification, the temperature response to changes in atmospheric CO_2 is generally larger over Greenland compared to the global mean. Specifically, the Greenland summer temperature change is a factor ∼1.2 larger than the mean global annual temperature change (Supplementary Fig. S5), which is consistent with the relation of 1.19±0.3 found in other Earth system models [33].

On multi-millennial time-scales, it is additionally important to account for the impact that changes in orbital parameters have on regional and seasonal climate. Over the next 10,000 years, a change in Earth's orbital parameters leads to an increase in summer insolation at high northern latitudes (Extended Data Fig. 1c), which results in summer temperatures over Greenland that are up to ∼1°C higher than under present-day orbital parameters (Fig. 4a,e, Supplementary Fig. S4d-f), while global annual temperatures are almost unchanged (Fig. 4a). In our simulations, up to ∼1.5 m of

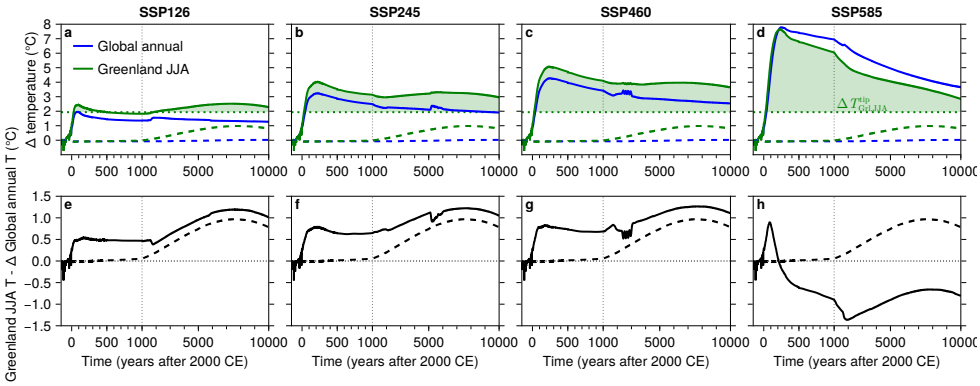

Fig. 4 Global vs Greenland temperature evolution. **a-d** Simulated evolution of the global annual temperature (blue) and the Greenland summer (JJA) temperature (green) over the next 10,000 years for different SSP scenarios and the reference ECS. The dashed lines indicate the natural evolution in the absence of anthropogenic forcings. The shaded green area indicates the temperature above the tipping point of the GrIS in terms of Greenland summer temperature ($\Delta T^{\mathrm{tip}}_{\mathrm{Grl,JJA}}$ ≈1.9°C, dotted green line) in the model. The results are from model simulations with a prescribed present-day GrIS. **e-h** Difference between Greenland summer temperature and global annual temperature for the different SSP scenarios (solid) and for the case without anthropogenic forcings (dashed). The qualitatively different relation between global and Greenland temperatures in **d,h** is due to a simulated shutdown of the Atlantic meridional overturning circulation in SSP585.

sea-level rise at the end of the simulations can be attributed to the changing Earth's orbital parameters, with the impact being generally larger under low-to-intermediate emission scenarios (Extended Data Fig. 5).

As noted above, the critical peak global warming above which the GrIS starts to show substantial ice loss is higher at 1,000 years compared to 10,000 years into the future (∼3°C and ∼1.5°C respectively; Fig. 2a, Extended Data Fig. 6a). This difference can be mainly attributed to the changes in orbital parameters and their prominent effect on Greenland and global temperatures beyond a few millennia in the future (Fig. 4). If the orbital parameters are kept constant at their present-day values, the critical peak global warming level ($\Delta T^{\mathrm{crit}}_{\mathrm{peak}}$) shifts higher by ∼1°C to $\Delta T^{\mathrm{crit}}_{\mathrm{peak,fixorb}}$ =∼2.5°C (Fig. 2b, Extended Data Fig. 6b). Future orbital forcing therefore acts to decrease the 'safe' peak global warming level for the GrIS by ∼1°C.

2.4 Relation with stability diagram

The stability diagram of the GrIS is often presented to show the presence of a tipping-point in the GrIS response to warming. In our model, the global warming threshold above which the GrIS is completely lost in quasi-equilibrium experiments with different constant CO_2 levels and present-day orbital parameters is $\Delta T^{\mathrm{tip}}_{\mathrm{glob}}$ ≈1.6°C (Fig. 5), which falls within the previously estimated GrIS tipping-point range of ∼1–3°C of global warming [27, 31–34]. This tipping point is somewhat sensitive to model parameters, particularly to surface mass balance parameters (Fig. 5). Additionally, in some

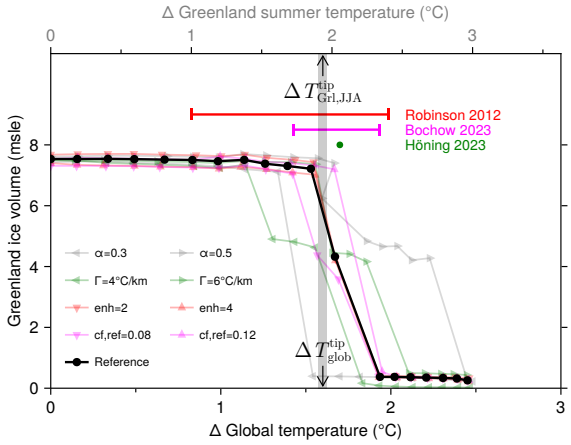

Fig. 5 Stability diagram of the GrIS. Equilibrium GrIS volume as a function of warming relative to pre-industrial derived from 100,000 years long simulations for different prescribed constant CO_2 levels and present-day orbital parameters in the CLIMBER-X reference simulations (black) and for the perturbed parameters ensemble (colored markers and lines). Greenland summer temperature change is shown as an additional x-axis on top, using the relation between global annual temperature change and Greenland summer temperature change shown in Supplementary Fig. S5. The abrupt decrease in ice volume above ∼1.6°C global warming shows the bifurcation (or tipping) point of the GrIS. Some previous estimates of the critical warming level leading to a complete loss of the GrIS are also shown at the top: in red from ref. [32] and in magenta from ref. [33], both originally defined by the Greenland summer temperature, and in green from ref. [27], originally defined by global temperature.

cases an intermediate GrIS state with ∼4.5 msle is stable for a range of global warming. Intermediate states of the GrIS have also been found in previous studies [27, 32, 48].

Since this stability diagram in global temperature space is derived for present-day orbital parameters, it is useful mainly for the interpretation of the future GrIS evolution in our idealised simulations with fixed orbit. The diagram clearly shows that, in the absence of orbital forcing, the GrIS could withstand a temporary global temperature overshoot of ∼1°C ($\Delta T^{crit}_{peak,fixorb} - \Delta T^{tip}_{glob}$) relative to its tipping-point temperature without a significant mass loss (Fig. 2b). This resilience of the GrIS to a temporary temperature overshoot is a result of the long time scale associated with the ice-sheet response to warming [49] and is consistent with recent studies using idealised carbon emissions or global warming scenarios, where it was found that centennial-scale overshoots of the critical temperature threshold do not necessarily lead to substantial ice loss [27, 33].

In the context of the long-term future evolution of the GrIS, when changing orbital parameters become important, the stability diagram in Greenland summer temperature space is more appropriate as it also accounts for the effect of regional and seasonal insolation changes. The tipping-point in terms of Greenland summer temperature is $\Delta T^{tip}_{Grl,JJA} \approx 1.9$°C (Fig. 5), again consistent with previous studies that found values between 1.0 and 2.4°C [32] or 1.8 and 2.5°C [33]. In our model, there is a tight linear relationship between the GrIS volume in 10,000 years and the average overshoot of $\Delta T^{tip}_{Grl,JJA}$ (Extended Data Fig. 7a). As a rule of thumb, the loss of half of the

GrIS within the next 10,000 years requires an average temperature exceedance of the tipping-point by ∼1.2°C, while a complete melting of the GrIS requires temperatures on average by ∼2°C higher than the tipping-point (Extended Data Fig. 7a).

3 Discussion

The results of coupled climate–carbon cycle–GrIS model simulations for the next 10,000 years under different future emission scenarios show that the long-term mass loss from the GrIS in 10,000 years can be predicted from peak global warming (ΔT_{peak}), which is expected to be reached within the next few centuries. If peak warming is below $\Delta T^{\mathrm{crit}}_{\mathrm{peak}}$ ≈1.5°C, the ice sheet will remain stable over this time period, and would only show a weak linear response to warming. However, each degree of peak warming above this threshold will cause ∼1.5 metres sea-level rise (SLR) from GrIS melt in 10,000 years:

$$SLR_{10\mathrm{kyr}} = \begin{cases} SLR^{\mathrm{nat}}_{10\mathrm{kyr}} + 0.2 \cdot \Delta T_{\mathrm{peak}} & \text{if } \Delta T_{\mathrm{peak}} \leq \Delta T^{\mathrm{crit}}_{\mathrm{peak}} \\ SLR^{\mathrm{nat}}_{10\mathrm{kyr}} + 0.2 \cdot \Delta T^{\mathrm{crit}}_{\mathrm{peak}} + 1.5 \cdot \left(\Delta T_{\mathrm{peak}} - \Delta T^{\mathrm{crit}}_{\mathrm{peak}}\right) & \text{if } \Delta T_{\mathrm{peak}} > \Delta T^{\mathrm{crit}}_{\mathrm{peak}}, \end{cases} \quad (1)$$

with $SLR^{\mathrm{nat}}_{10\mathrm{kyr}} \approx 0.2$ being the natural sea level rise in 10,000 years originating from the changing Earth's orbital parameters alone. The fact that this emerging piecewise linear relation holds across different emission scenarios and ECS is noteworthy and substantially reduces the number of degrees of freedom for assessing the long-term GrIS response to global warming.

A number of studies have shown a relation between Greenland ice loss and temperature change in the short-term [11] and in the long-term [25, 50]. The fact that the long-term ice loss in our simulations can be predicted from the short-term peak warming relies on a robust relation between peak global warming and the average temperature overshoot of the Greenland tipping point temperature $\Delta T^{\mathrm{tip}}_{\mathrm{Grl,JJA}}$ ≈1.9°C (Fig. 4a-d and Extended Data Fig. 7b), which is valid as long as the negative carbon emissions are temporary and limited, as is the case for the considered SSP scenarios. A more aggressive and persistent deployment of carbon capture and storage technologies, such as in the overshoot scenario SSP534-over, would decrease global temperatures more rapidly after peak warming (Extended Data Fig. 8), affecting the relation between short-term and long-term temperatures (Extended Data Fig. 7d). Nevertheless, while the results for the overshoot scenario clearly deviate from the other considered SSP scenarios, they are still reasonably close to the relation shown in Eq. 1 (Extended Data Fig. 9), suggesting that these results are actually relatively robust even to scenarios with large, but temporally limited, CO_2 removal.

Our findings also help to relate the long-term GrIS response to the GrIS tipping point. The critical peak warming level above which significant long-term (10,000 years) GrIS mass loss occurs ($\Delta T^{\mathrm{crit}}_{\mathrm{peak}}$ ∼1.5°C) is very close to the equilibrium tipping point temperature of the GrIS ($\Delta T^{\mathrm{tip}}_{\mathrm{glob}}$ ∼1.6°C). This is not trivial; it is the result of the resilience of the GrIS to temporary temperature overshoots [33, 49] being compensated by enhanced melt following the increasing summer insolation at high northern latitudes due to changing orbital parameters. For the multi-millennial future evolution and

stability of the GrIS it is therefore important to account for the effect of changes in Earth's orbit.

Although peak temperature has yet to be realised, this work demonstrates how 21st century climate policy can have long-lasting consequences, with decisions made today potentially driving the evolution of the GrIS for millennia to come.

4 Methods

4.1 Earth system model

We use the fast Earth system model CLIMBER-X [41–43], including the frictional-geostrophic 3D ocean model GOLDSTEIN [51, 52] with 23 vertical layers, the semi-empirical statistical-dynamical atmosphere model SESAM [41], the dynamic-thermodynamic sea-ice model SISIM [41], the land-surface model with interactive vegetation PALADYN [53] and the ocean biogeochemistry model HAMOCC6 [54–56]. The comprehensive carbon cycle in the model computes the atmospheric CO_2 and CH_4 evolution interactively, while accounting for slow processes associated with permafrost, marine sediments and chemical rock weathering, which are important on millennial time scales [20, 57]. All components of the climate model have a horizontal resolution of 5°×5°. The dynamics of the GrIS is represented by the ice-sheet model Yelmo [44], coupled to the climate model via the physically-based surface energy and mass balance interface SEMIX [43]. To solve for dynamics, Yelmo uses the higher-order Depth Integrated Viscosity Approximation (DIVA), interactive thermodynamics, a local (bucket) basal hydrology model with a till drainage rate of 0.008 m/yr and effective pressure, N, calculated as a function of the thickness of the basal water layer [58]. Basal friction is represented with a regularized Coulomb sliding law,

$$\tau_b = c_f N \left(\frac{|\mathbf{u}_b|}{|\mathbf{u}_b| + u_0} \right)^q \frac{\mathbf{u}_b}{|\mathbf{u}_b|} \tag{2}$$

where u_0=100 m/yr and q=0.2, and c_f is a non-dimensional, spatially variable field that represents bedrock/till properties, defined as:

$$c_f = \begin{cases} c_{\mathrm{f,ref}}, & \text{if } z_b > z_1, \\ \max\left(c_{\mathrm{f,ref}} \cdot \exp\left(\frac{z_b - z_1}{z_1 - z_0} \right),\ c_{\mathrm{f,min}} \right), & \text{otherwise}, \end{cases} \tag{3}$$

where $c_{\mathrm{f,ref}}$=0.1, $c_{\mathrm{f,min}}$=0.01, z_1=100 m and z_0=-100 m and z_b is the bedrock elevation. In this way, the friction coefficient becomes lower at lower elevations and varies between $c_{\mathrm{f,ref}}$ and $c_{\mathrm{f,min}}$. We employ a parameterisation of sub-grid ice discharge into the ocean for unresolved narrow outlet glaciers dynamics [59]. The horizontal resolution of the ice-sheet model in the reference runs is 8 km, which is comparable to resolutions typically employed in stand-alone GrIS modeling studies [13]. Sensitivity tests using 16 and 32 km indicate that results are converging for resolutions finer than ∼16 km (Supplementary Fig. S7 and Supplementary Fig. S8), which is fully consistent with previous results [24]. The viscoelastic solid Earth model VILMA [60–62] computes the glacial isostatic adjustment and relative sea-level changes. For simplicity, Antarctica is prescribed at its modern state. The climate model is described in detail in ref. [41], the carbon cycle model in ref. [42] and the ice-sheet coupling in ref. [43].

4.2 Ensemble with different climate sensitivities

The GrIS is known to be very sensitive to changes in climate, and in particular to the air temperature during the summer season. Since the projected future temperature evolution strongly depends on the poorly constrained ECS, in this study we use an ensemble of CLIMBER-X simulations with different ECS following ref. [46] to cover the broad range of uncertainties in the climate response to anthropogenic forcings.

We mimic different ECS in the model by scaling the radiative forcing of equivalent atmospheric CO_2 concentration and at the same time adjust the (negative) aerosol forcing to match the historical temperature trends. A more detailed description of how the ECS ensemble is generated is provided by ref. [46].

Ref. [46] have already shown that this approach works well in covering the range of expected global warming levels, with differences in ECS among CMIP6 models largely explaining the differences in future predicted global warming (Supplementary Fig. S1a). Here we additionally show that our ECS-scaling approach also performs well for the regional summer warming over Greenland (Supplementary Fig. S1), which is the crucial climate variable controlling the surface mass balance of the ice sheet. We are therefore confident that our ensemble with different ECS spans the uncertainty range in future Greenland warming related to the uncertainties in ECS.

4.3 Sensitivity to model parameters

To further investigate the sensitivity of our results to uncertain model parameters directly related to the representation of the GrIS we have created a perturbed parameter ensemble, which complements the ECS ensemble described above. We perturbed surface mass balance scheme parameters (bare ice albedo (α) values of 0.3 and 0.5 compared to the default 0.4, and temperature lapse rate (Γ) values of 4°C/km and 6°C/km compared to the default of 5°C/km), and ice sheet model parameters (flow enhancement factor values of 2 and 4 compared to the default of 3, and a perturbation by $\pm 20\%$ to the reference basal friction coefficient $c_{\mathrm{f,ref}}$).

4.4 Model evaluation

In general, CLIMBER-X shows performance on many metrics that is comparable with state-of-the-art CMIP6 models under different forcings and boundary conditions [41, 42]. The model ensemble with different ECS reproduces the historical changes in temperature and CO_2 and CH_4 concentrations [46] (Supplementary Fig. S2 and Fig. S3).

Specifically for Greenland, the relation between simulated summer temperature change and global temperature change in future scenarios compares well with results from CMIP6 models (Supplementary Fig. S1). The non-linear dependence of surface mass balance of the GrIS to changes in temperature is also well captured by the CLIMBER-X model, when compared to simulations from regional climate models [12, 63] (Extended Data Fig. 3), providing support for the realistic response of the surface mass balance to climate change in our model.

The simulated GrIS under pre-industrial equilibrium conditions agrees reasonably well with present-day observations (Fig. 2). The total simulated ice volume is

~7.5 msle, and therefore somewhat larger than the estimated 7.4 msle [1], mainly as the modelled ice sheets are thicker in the western part. The model also reproduces the large-scale surface ice velocity patterns for the GrIS reasonably well, including prominent fast-flowing regions (Fig. 2).

4.5 Experiments

Starting from the pre-industrial period, we performed model simulations into the future using 6 different SSP scenarios [45], namely SSP119, SSP126, SSP245, SSP460, SSP370 and SSP585.

For the historical period we apply standard forcings used also in the CMIP6 model simulations, as described in ref. [41] and ref. [42]. Since our model simulations are emission driven (for both CO_2 and CH_4), anthropogenic CO_2 and CH_4 emissions are prescribed instead of their concentrations.

Future anthropogenic CO_2 emissions are prescribed from ref. [45] until the year 2500 CE, with zero emissions assumed afterwards. Anthropogenic CH_4 emissions are prescribed from ref. [64] for the historical period, and from ref. [65] for the future. Emission scenarios end at 2100 CE and have been extended following ref. [45] and ref. [66], with a linear decrease of non-agricultural emissions to zero by 2250 CE. Emissions from agricultural sources stay constantly elevated beyond this time. Anthropogenic N_2O concentrations are prescribed from ref. [45] until the year 2500 CE, and are kept constant thereafter. Land use change is prescribed following ref. [67] until the year 2100 CE, and is kept constant afterwards. The 2D anomalies of SO_4^{2-} atmospheric load relative to pre-industrial from the ensemble mean of CMIP6 models are applied for the historical period, and for the different SSP scenarios until 2100 CE. After 2100 CE, the anomaly in SO_4^{2-} loading is anticipated to diminish, and is described by a linear decrease to zero by 2250 CE. The 3D O_3 concentration from the ensemble mean of CMIP6 models is prescribed for the historical period, and kept constant afterwards.

For multi-millennial time scales, changes in the orbital configuration of the Earth around the Sun are important and therefore explicitly considered in our experiments [68]. To test the role of changes in the orbital parameters for the future evolution of the GrIS, we additionally repeated the SSP experiments with prescribed constant present-day orbital parameters.

All external forcings applied to the model are shown in Extended Data Fig. 1.

All model simulations are initialised from a pre-industrial equilibrium state that is obtained from a 100,000 year equilibrium spinup procedure of the carbon cycle as described in ref. [42]. Additionally, the GrIS is equilibrated with the pre-industrial climate in a spinup over 50,000 years starting from the present-day observed ice-sheet state and an initial uniform ice temperature of -10°C. The ice-sheet spinup is performed using a climate acceleration factor of 10. Since the ECS scaling procedure and the aerosol forcing do not affect the pre-industrial climate, the pre-industrial equilibrium state is the same for all ensemble members with different ECS. Separate spinup simulations are performed for the perturbed parameter ensemble.

To determine the tipping point temperature above which the GrIS is not stable and completely melts in the model we performed a set of equilibrium (100,000 years) simulations with prescribed constant CO_2 concentrations between 280 and 460 ppm,

sampled at steps of 10 ppm. This set of simulations used an acceleration factor of 10 for the climate component.

To derive the relation between global temperature change and regional summer temperature change over Greenland in the model, we performed equilibrium simulations of 5,000 years with constant CO_2 levels and a prescribed present-day GrIS state. We considered CO_2 concentrations between 280 and 460 ppm, at steps of 10 ppm. We also ran a simulation with fixed present-day ice sheets for the SSP245 scenario, in order to compare the relation between ECS, global temperature and Greenland summer temperature with CMIP6 models (Supplementary Fig. S1).

To determine the effect of changes in the orbital conditions on the summer temperatures over Greenland, we ran transient simulations with prescribed present-day GrIS for natural conditions and for all extended SSP scenarios. This set of experiments was performed only for the reference ECS.

To address the robustness of the results to extreme overshoot scenarios, We additionally ran a set of simulations for the overshoot scenario SSP534-over.

A list of all performed model simulations is provided in Extended Data Table 1. All together the simulations amount to 8 million simulation years for the climate model and 29 million simulation years for the ice sheet model.

Acknowledgements. MW is funded by the German climate modelling project PalMod supported by the German Federal Ministry of Education and Research (BMBF) as a Research for Sustainability initiative (FONA) (grant nos. 01LP1920B, 01LP1917D, 01LP2305B) and by the P2F project. The Past to Future (P2F) project has received funding from the European Union's Horizon Europe research and innovation programme under grant agreement No. 101184070: Funded by the European Union. CK is funded by the Bundesgesellschaft für Endlagerung through the URS project (research project no. STAFuE-21-4-Klei). AR received funding from the European Research Council (ERC Consolidator grant, FORCLIMA, grant no. 101044247). This is ClimTip contribution #XX; the ClimTip project has received funding from the European Union's Horizon Europe research and innovation programme under grant agreement No. 101137601: Funded by the European Union. Views and opinions expressed are however those of the author(s) only and do not necessarily reflect those of the European Union or the European Climate, Infrastructure and Environment Executive Agency (CINEA). Neither the European Union nor the granting authority can be held responsible for them. The authors gratefully acknowledge the European Regional Development Fund (ERDF), the German Federal Ministry of Education and Research and the Land Brandenburg for supporting this project by providing resources on the high performance computer system at the Potsdam Institute for Climate Impact Research.

Declarations

Competing interests. The authors declare no competing interests.

Data availability. The output of the model simulations is available on Zenodo at: https://doi.org/10.5281/zenodo.17510554.

Code availability. The CLIMBER-X model code is available at https://github.com/cxesmc/climber-x. For this study we used the tagged version v1.4.3grl of the model.

Author contribution. M.W. conceived and designed the study. M.W. and A.R. set up the model configurations and M.W. performed the model simulations. M.W. and C.K. prepared the figures. All authors contributed to the analysis and discussion of the results and the writing of the paper.

References

[1] Morlighem, M. *et al.* BedMachine v3: Complete Bed Topography and Ocean Bathymetry Mapping of Greenland From Multibeam Echo Sounding Combined With Mass Conservation. *Geophysical Research Letters* **44**, 11,051–11,061 (2017).

[2] Fox-Kemper, B. *et al.* in *Chapter 9: Ocean, Cryosphere and Sea Level Change* (eds Masson-Delmotte, V. *et al.*) *Climate Change 2021: The Physical Science Basis. Contribution of Working Group I to the Sixth Assessment Report of the Intergovernmental Panel on Climate Change* 1211–1361 (Cambridge University Press, Cambridge, UK and New York, NY, USA, 2021).

[3] Mouginot, J. *et al.* Forty-six years of Greenland Ice Sheet mass balance from 1972 to 2018. *Proceedings of the National Academy of Sciences of the United States of America* **116**, 9239–9244 (2019).

[4] Mankoff, K. D. *et al.* Greenland Ice Sheet solid ice discharge from 1986 through March 2020. *Earth System Science Data* **12**, 1367–1383 (2020).

[5] Shepherd, A. *et al.* Mass balance of the Greenland Ice Sheet from 1992 to 2018. *Nature* **579**, 233–239 (2020).

[6] Mankoff, K. D. *et al.* Greenland ice sheet mass balance from 1840 through next week. *Earth System Science Data* **13**, 5001–5025 (2021).

[7] Box, J. E. *et al.* Greenland ice sheet climate disequilibrium and committed sea-level rise. *Nature Climate Change* **12** (2022).

[8] Otosaka, I. N. *et al.* Mass balance of the Greenland and Antarctic ice sheets from 1992 to 2020. *Earth System Science Data* **15**, 1597–1616 (2023).

[9] Calov, R. *et al.* Simulation of the future sea level contribution of Greenland with a new glacial system model. *Cryosphere* **12**, 3097–3121 (2018).

[10] Golledge, N. R. *et al.* Global environmental consequences of twenty-first-century ice-sheet melt. *Nature* **566**, 65–72 (2019). URL http://dx.doi.org/10.1038/s41586-019-0889-9.

[11] Edwards, T. L. *et al.* Projected land ice contributions to twenty-first-century sea level rise. *Nature* **593**, 74–82 (2021).

[12] Noël, B., van Kampenhout, L., Lenaerts, J. T., van de Berg, W. J. & van den Broeke, M. R. A 21st Century Warming Threshold for Sustained Greenland Ice Sheet Mass Loss. *Geophysical Research Letters* **48**, 1–9 (2021).

[13] Goelzer, H. *et al.* The future sea-level contribution of the Greenland ice sheet: A multi-model ensemble study of ISMIP6. *Cryosphere* **14**, 3071–3096 (2020).

[14] Vizcaino, M. *et al.* Coupled simulations of Greenland Ice Sheet and climate change up to A.D. 2300. *Geophysical Research Letters* **42**, 3927–3935 (2015). URL https://agupubs.onlinelibrary.wiley.com/doi/10.1002/2014GL061142.

[15] Muntjewerf, L. *et al.* Greenland Ice Sheet Contribution to 21st Century Sea Level Rise as Simulated by the Coupled CESM2.1-CISM2.1. *Geophysical Research Letters* **47** (2020).

[16] Park, J. Y. *et al.* Future sea-level projections with a coupled atmosphere-ocean-ice-sheet model. *Nature Communications* **14** (2023).

[17] Haubner, K., Goelzer, H. & Born, A. Limited global effect of climate-Greenland ice sheet coupling in NorESM2 under a high-emission scenario. *Earth System Dynamics* **17**, 57–80 (2026).

[18] Archer, D. Fate of fossil fuel CO_2 in geologic time. *Journal of Geophysical Research: Oceans* **110**, 1–6 (2005).

[19] Lord, N. S., Ridgwell, A., Thorne, M. C. & Lunt, D. J. An impulse response function for the "long tail" of excess atmospheric CO_2 in an Earth system model. *Global Biogeochemical Cycles* **30**, 2–17 (2016). URL https://agupubs.onlinelibrary.wiley.com/doi/10.1002/2014GB005074.

[20] Kaufhold, C., Willeit, M., Liu, B. & Ganopolski, A. Assessing the lifetime of anthropogenic CO_2 and its sensitivity to different carbon cycle processes. *Biogeosciences* **22**, 2767–2801 (2025).

[21] Charbit, S., Paillard, D. & Ramstein, G. Amount of CO_2 emissions irreversibly leading to the total melting of Greenland. *Geophysical Research Letters* **35**, 1–5 (2008).

[22] Huybrechts, P. *et al.* Response of the Greenland and Antarctic Ice Sheets to Multi-Millennial Greenhouse Warming in the Earth System Model of Intermediate Complexity LOVECLIM. *Surveys in Geophysics* **32**, 397–416 (2011). URL http://link.springer.com/10.1007/s10712-011-9131-5.

[23] Gregory, J. M., George, S. E. & Smith, R. S. Large and irreversible future decline of the Greenland ice sheet. *The Cryosphere* **14**, 4299–4322 (2020).

[24] Aschwanden, A. *et al.* Contribution of the Greenland Ice Sheet to sea level over the next millennium. *Science Advances* **5** (2019).

[25] Clark, P. U. *et al.* Consequences of twenty-first-century policy for multi-millennial climate and sea-level change. *Nature Climate Change* **6**, 360–369 (2016).

[26] Van Breedam, J., Goelzer, H. & Huybrechts, P. Semi-equilibrated global sea-level change projections for the next 10 000 years. *Earth System Dynamics* **11**,

953–976 (2020).

[27] Höning, D. *et al.* Multistability and Transient Response of the Greenland Ice Sheet to Anthropogenic CO_2 Emissions. *Geophysical Research Letters* **50**, 1–11 (2023).

[28] Paice, C. M., Fettweis, X. & Huybrechts, P. Positive feedbacks drive the Greenland ice sheet evolution in millennial-length MAR–GISM simulations under a high-end warming scenario. *The Cryosphere* **20**, 309–332 (2026).

[29] Ridley, J., Gregory, J. M., Huybrechts, P. & Lowe, J. Thresholds for irreversible decline of the Greenland ice sheet. *Climate Dynamics* **35**, 1065–1073 (2010).

[30] Höning, D., Willeit, M. & Ganopolski, A. Reversibility of Greenland ice sheet mass loss under artificial carbon dioxide removal scenarios. *Environmental Research Letters* **19** (2024).

[31] Gregory, J. & Huybrechts, P. Ice-sheet contributions to future sea-level change. *Philosophical Transactions of the Royal Society A: Mathematical, Physical and Engineering Sciences* **364**, 1709–1732 (2006). URL https://royalsocietypublishing.org/doi/10.1098/rsta.2006.1796.

[32] Robinson, A., Calov, R. & Ganopolski, A. Multistability and critical thresholds of the Greenland ice sheet. *Nature Climate Change* **2**, 429–432 (2012). URL http://www.nature.com/doifinder/10.1038/nclimate1449.

[33] Bochow, N. *et al.* Overshooting the critical threshold for the Greenland ice sheet. *Nature* **622**, 528–536 (2023). URL https://www.nature.com/articles/s41586-023-06503-9.

[34] Petrini, M. *et al.* A topographically controlled tipping point for complete Greenland ice sheet melt. *The Cryosphere* **19**, 63–81 (2025). URL https://tc.copernicus.org/articles/19/63/2025/.

[35] Pöppelmeier, F. & Stocker, T. F. Mutual stabilization of AMOC and GrIS due to different transient response to warming. *Environmental Research Letters* (2025).

[36] Lunt, D. J., Foster, G. L., Haywood, A. M. & Stone, E. J. Late Pliocene Greenland glaciation controlled by a decline in atmospheric CO_2 levels. *Nature* **454**, 1102–5 (2008). URL http://www.ncbi.nlm.nih.gov/pubmed/18756254.

[37] Dutton, A. *et al.* Sea-level rise due to polar ice-sheet mass loss during past warm periods. *Science* **349**, aaa4019– (2015). URL http://www.sciencemag.org/content/349/6244/aaa4019.abstract.

[38] Robinson, A., Alvarez-Solas, J., Calov, R., Ganopolski, A. & Montoya, M. MIS-11 duration key to disappearance of the Greenland ice sheet. *Nature*

Communications **8**, 1–7 (2017). URL http://dx.doi.org/10.1038/ncomms16008.

[39] Köhler, P., Nehrbass-Ahles, C., Schmitt, J., Stocker, T. F. & Fischer, H. A 156 kyr smoothed history of the atmospheric greenhouse gases CO_2, CH_4 and N_2O and their radiative forcing. *Earth System Science Data* **9**, 363–387 (2017). URL https://www.earth-syst-sci-data.net/9/363/2017/https://essd.copernicus.org/articles/9/363/2017/.

[40] Morice, C. P. *et al.* An Updated Assessment of Near-Surface Temperature Change From 1850: The HadCRUT5 Data Set. *Journal of Geophysical Research: Atmospheres* **126**, 1–28 (2021).

[41] Willeit, M., Ganopolski, A., Robinson, A. & Edwards, N. R. The Earth system model CLIMBER-X v1.0 – Part 1: Climate model description and validation. *Geoscientific Model Development* **15**, 5905–5948 (2022). URL https://gmd.copernicus.org/articles/15/5905/2022/.

[42] Willeit, M. *et al.* The Earth system model CLIMBER-X v1.0 – Part 2: The global carbon cycle. *Geoscientific Model Development* **16**, 3501–3534 (2023). URL https://doi.org/10.5194/gmd-2022-307https://gmd.copernicus.org/articles/16/3501/2023/.

[43] Willeit, M. *et al.* Glacial inception through rapid ice area increase driven by albedo and vegetation feedbacks. *Climate of the Past* **20**, 597–623 (2024). URL https://cp.copernicus.org/articles/20/597/2024/.

[44] Robinson, A. *et al.* Description and validation of the ice-sheet model Yelmo (version 1.0). *Geoscientific Model Development* **13**, 2805–2823 (2020).

[45] Meinshausen, M. *et al.* The shared socio-economic pathway (SSP) greenhouse gas concentrations and their extensions to 2500. *Geoscientific Model Development* **13**, 3571–3605 (2020).

[46] Kaufhold, C., Willeit, M., Talento, S., Ganopolski, A. & Rockström, J. Interplay between climate and carbon cycle feedbacks could substantially enhance future warming. *Environmental Research Letters* **20**, 044027 (2025). URL https://iopscience.iop.org/article/10.1088/1748-9326/adb6be.

[47] Pielke, R., Burgess, M. G. & Ritchie, J. Plausible 2005-2050 emissions scenarios project between 2 °c and 3 °c of warming by 2100. *Environmental Research Letters* **17** (2022).

[48] Andernach, M., Kapsch, M.-L. & Mikolajewicz, U. Stabilizing feedbacks allow for multiple states of the Greenland Ice Sheet in a fully coupled Earth System – Ice Sheet Model. *The Cryosphere* **20**, 1047–1069 (2026).

[49] Ritchie, P. D. L., Clarke, J. J., Cox, P. M. & Huntingford, C. Overshooting tipping point thresholds in a changing climate. *Nature* **592**, 517–523 (2021). URL http://dx.doi.org/10.1038/s41586-021-03263-2https://www.nature.com/articles/s41586-021-03263-2.

[50] Pattyn, F. *et al.* The Greenland and Antarctic ice sheets under 1.5 °C global warming. *Nature Climate Change* **8**, 1053–1061 (2018).

[51] Edwards, N. R., Willmott, A. J. & Killworth, P. D. On the Role of Topography and Wind Stress on the Stability of the Thermohaline Circulation. *Journal of Physical Oceanography* **28**, 756–778 (1998).

[52] Edwards, N. R. & Marsh, R. Uncertainties due to transport-parameter sensitivity in an efficient 3-D ocean-climate model. *Climate Dynamics* **24**, 415–433 (2005). URL http://link.springer.com/10.1007/s00382-004-0508-8.

[53] Willeit, M. & Ganopolski, A. PALADYN v1.0, a comprehensive land surface–vegetation–carbon cycle model of intermediate complexity. *Geoscientific Model Development* **9**, 3817–3857 (2016). URL http://www.geosci-model-dev-discuss.net/gmd-2016-92/http://www.geosci-model-dev.net/9/3817/2016/.

[54] Ilyina, T. *et al.* Global ocean biogeochemistry model HAMOCC: Model architecture and performance as component of the MPI-Earth system model in different CMIP5 experimental realizations. *Journal of Advances in Modeling Earth Systems* **5**, 287–315 (2013).

[55] Mauritsen, T. *et al.* Developments in the MPI-M Earth System Model version 1.2 (MPI-ESM1.2) and Its Response to Increasing CO_2. *Journal of Advances in Modeling Earth Systems* **11**, 998–1038 (2019).

[56] Liu, B., Six, K. D. & Ilyina, T. Incorporating the stable carbon isotope 13C in the ocean biogeochemical component of the Max Planck Institute Earth System Model. *Biogeosciences* **18**, 4389–4429 (2021).

[57] Kaufhold, C., Willeit, M., Munhoven, G., Klemann, V. & Ganopolski, A. Timing of a future glaciation in view of anthropogenic climate change. *Communications Earth & Environment* **6**, 1016 (2025).

[58] Bueler, E. & Van Pelt, W. Mass-conserving subglacial hydrology in the Parallel Ice Sheet Model version 0.6. *Geoscientific Model Development* **8**, 1613–1635 (2015).

[59] Calov, R., Robinson, a., Perrette, M. & Ganopolski, a. Simulating the Greenland ice sheet under present-day and palaeo constraints including a new discharge parameterization. *The Cryosphere* **9**, 179–196 (2015). URL http://www.the-cryosphere.net/9/179/2015/.

[60] Klemann, V., Martinec, Z. & Ivins, E. R. Glacial isostasy and plate motion. *Journal of Geodynamics* **46**, 95–103 (2008).

[61] Martinec, Z. *et al.* A benchmark study of numerical implementations of the sea level equation in GIA modelling. *Geophysical Journal International* **215**, 389–414 (2018).

[62] Bagge, M., Klemann, V., Steinberger, B., Latinović, M. & Thomas, M. Glacial-Isostatic Adjustment Models Using Geodynamically Constrained 3D Earth Structures. *Geochemistry, Geophysics, Geosystems* **22**, 1–21 (2021).

[63] Hofer, S. *et al.* Greater Greenland Ice Sheet contribution to global sea level rise in CMIP6. *Nature Communications* **11**, 1–11 (2020). URL http://dx.doi.org/10.1038/s41467-020-20011-8.

[64] Hoesly, R. M. *et al.* Historical (1750–2014) anthropogenic emissions of reactive gases and aerosols from the Community Emissions Data System (CEDS). *Geoscientific Model Development* **11**, 369–408 (2018). URL https://gmd.copernicus.org/articles/11/369/2018/.

[65] Gidden, M. J. *et al.* Global emissions pathways under different socioeconomic scenarios for use in CMIP6: A dataset of harmonized emissions trajectories through the end of the century. *Geoscientific Model Development* **12**, 1443–1475 (2019).

[66] Kleinen, T., Gromov, S., Steil, B. & Brovkin, V. Atmospheric methane underestimated in future climate projections. *Environmental Research Letters* **16** (2021).

[67] Ma, L. *et al.* Global rules for translating land-use change (LUH2) to land-cover change for CMIP6 using GLM2. *Geoscientific Model Development* **13**, 3203–3220 (2020). URL https://gmd.copernicus.org/articles/13/3203/2020/.

[68] Laskar, J. *et al.* A long-term numerical solution for the insolation quantities of the Earth. *Astronomy and Astrophysics* **428**, 261–285 (2004). URL http://www.edpsciences.org/10.1051/0004-6361:20041335.

[69] Schaffer, J. *et al.* A global, high-resolution data set of ice sheet topography, cavity geometry, and ocean bathymetry (2016).

[70] Joughin, I., Smith, B. E. & Howat, I. Greenland Ice Mapping Project: Ice flow velocity variation at sub-monthly to decadal timescales. *The Cryosphere* **12**, 2211–2227 (2018).

Extended Data Table 1 List of the performed CLIMBER-X experiments. The 6 SSP scenarios include SSP119, SSP126, SSP245, SSP370, SSP460 and SSP585. In total the simulations amount to 8 million simulation years for the climate model and 29 million simulation years for the ice sheet model.

Control and natural scenarios							
Simulation	**Model par**	**Forcings**	**ECS**	**GrIS**	**Orbital par**	**Simulation years**	**#Runs**
Control	Ref.	None	3°C	interactive 8 km	fixed PI	11,000 climate 11,000 ice sheet	1
Natural Ref	Ref.	None	3°C	interactive 8 km	variable	11,000 climate 11,000 ice sheet	1
Natural par sens	α=0.3 α=0.5 Γ=4°C km^{-1} Γ=6°C km^{-1} enh=2 enh=4 cf,ref=0.08 cf,ref=0.12	None	3°C	interactive 8 km	variable	11,000 climate 11,000 ice sheet	8
SSP scenarios							
Simulation	**Model par**	**Scenarios**	**ECS**	**GrIS**	**Orbital par**	**Simulation years**	**#Runs**
SSP Ref	Ref.	6 SSPs	2–5°C	interactive 8 km	variable	11,000 climate 11,000 ice sheet	42
SSP fix orb	Ref.	6 SSPs	3°C	interactive 8 km	fixed PI	11,000 climate 11,000 ice sheet	6
SSP fix ice	Ref.	6 SSPs	3°C	fixed PI	variable	11,000 climate	6
SSP 16 km	Ref.	6 SSPs	2–5°C	interactive 16 km	variable	11,000 climate 11,000 ice sheet	42
SSP 32 km	Ref.	6 SSPs	2–5°C	interactive 32 km	variable	11,000 climate 11,000 ice sheet	42
SSP par sens	α=0.3 α=0.5 Γ=4°C km^{-1} Γ=6°C km^{-1} enh=2 enh=4 cf,ref=0.08 cf,ref=0.12	6 SSPs	2–5°C	interactive 8 km	variable	11,000 climate 11,000 ice sheet	336
SSP over	Ref.	SSP534-over	2–5°C	interactive 8 km	variable	11,000 climate 11,000 ice sheet	7
Equilibrium CO_2							
Simulation	**Model par**	**CO_2**	**ECS**	**GrIS**	**Orbital par**	**Simulation years**	**#Runs**
EQ Ref	Ref.	280:10:460	3°C	interactive 8 km	fixed PI	10,000 climate 100,000 ice sheet	19
EQ fix ice	Ref.	280:10:460	3°C	fixed PI	fixed PI	10,000 climate	19
EQ 16 km	Ref.	280:10:460	3°C	interactive 16 km	fixed PI	10,000 climate 100,000 ice sheet	19
EQ 32 km	Ref.	280:10:460	3°C	interactive 32 km	fixed PI	10,000 climate 100,000 ice sheet	19
EQ par sens	α=0.3 α=0.5 Γ=4°C km^{-1} Γ=6°C km^{-1} enh=2 enh=4 cf,ref=0.08 cf,ref=0.12	280:10:460	3°C	interactive 8 km	fixed PI	10,000 climate 100,000 ice sheet	152

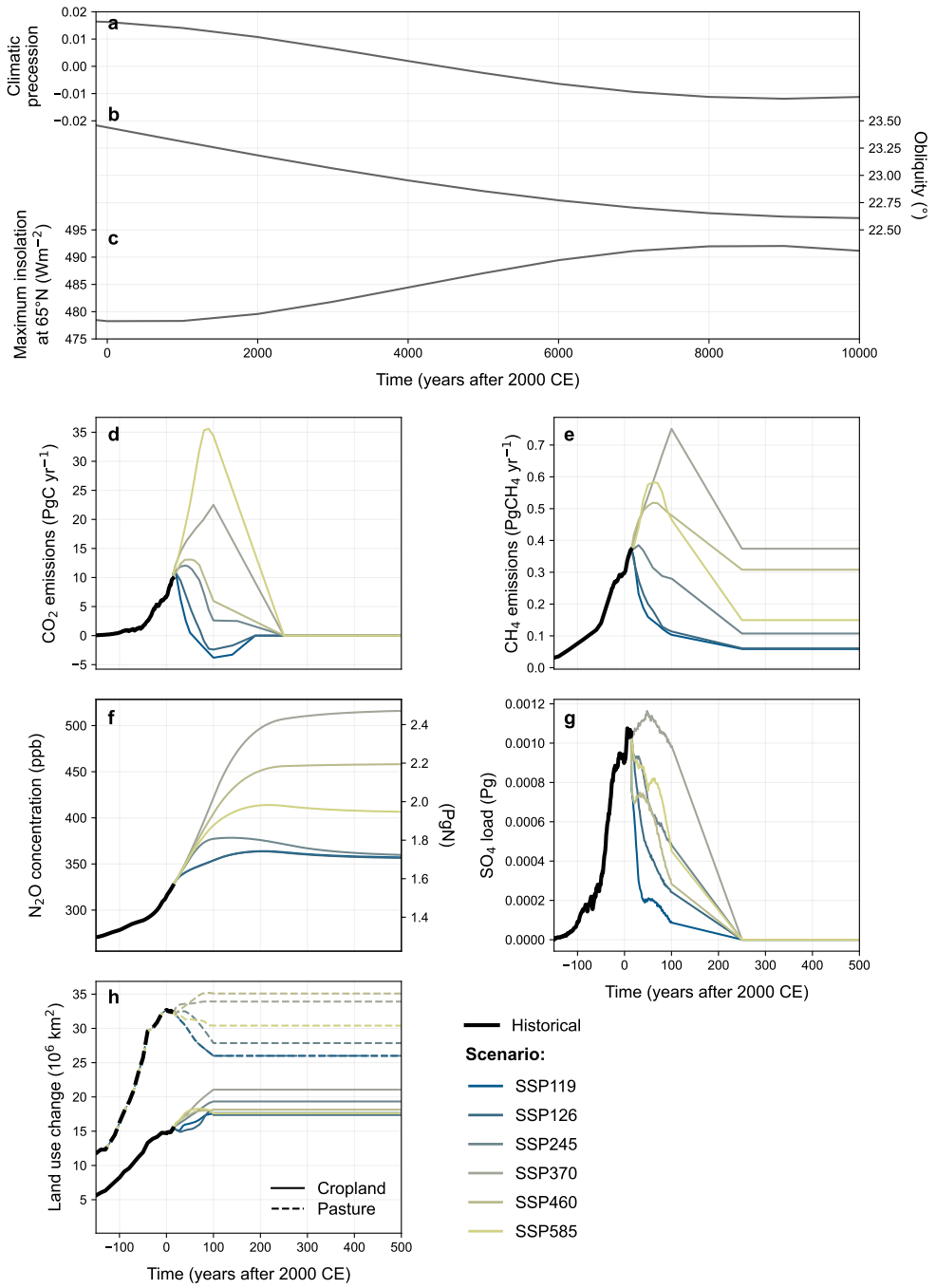

Extended Data Fig. 1 Forcings for the model simulations. a Climatic precession, **b** obliquity and **c** the resulting maximum summer insolation at 65°N [68]. **d** Anthropogenic CO_2 emissions [45]. **e** Anthropogenic CH_4 emissions [64, 65]. **f** N_2O concentrations [45]. **g** Global SO_4^{2-} load. **h** Global cropland and pasture areas [67].

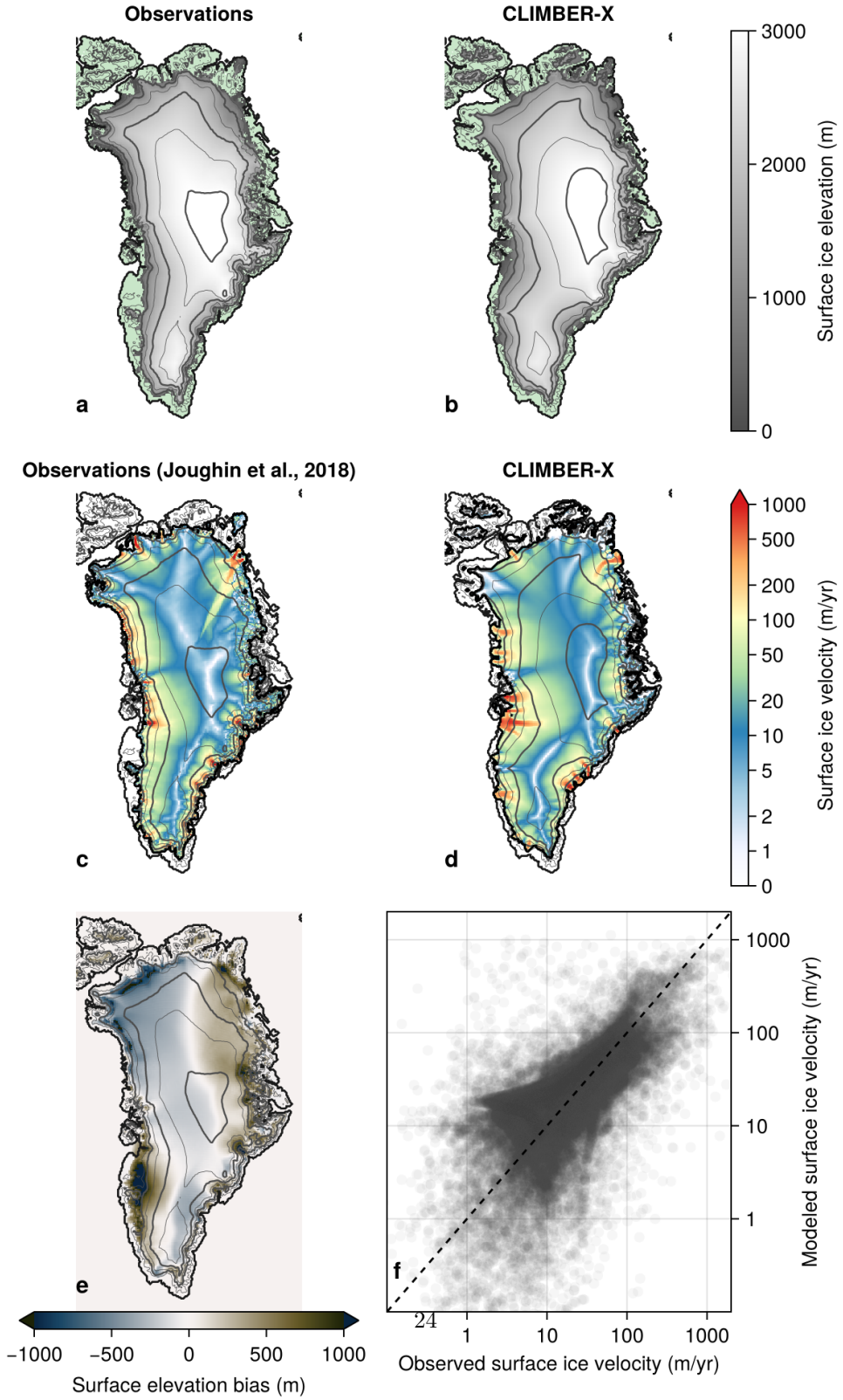

Extended Data Fig. 2 Present-day simulated GrIS compared to observations. a,b Comparison of simulated and observed [69] ice surface elevation and ice sheet extent. **c,d** Comparison of simulated and observed [70] surface ice velocities. **e** Deviation of simulated surface elevation from observations. **f** Modelled versus observed [70] surface ice velocities. The elevation contour lines shown in the different panels are spaced by 500 m, with the thick contour lines representing the 0, 1000, 2000 and 3000 m elevation isolines.

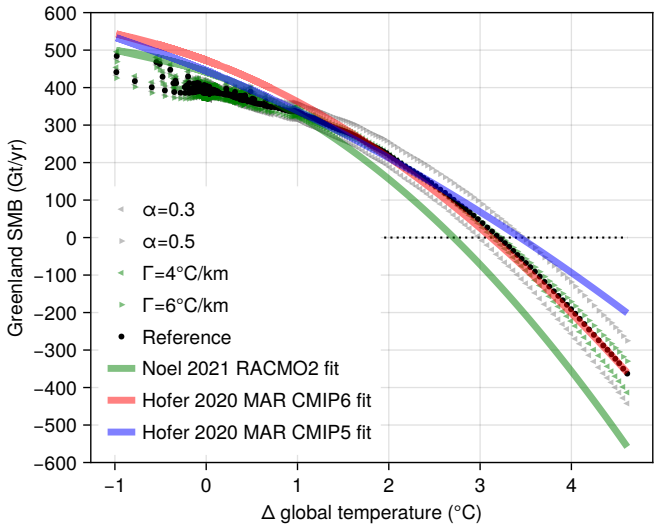

Extended Data Fig. 3 Greenland surface mass balance sensitivity to temperature. Relation between the surface mass balance of the GrIS and global temperature change from simulations of the SSP585 scenario until 2100 CE for CLIMBER-X compared to results from regional climate models [12, 63]. In addition to the reference model simulation, also the results for the different surface mass balance model parameters (α is the bare ice albedo and Γ is the temperature lapse rate) are shown.

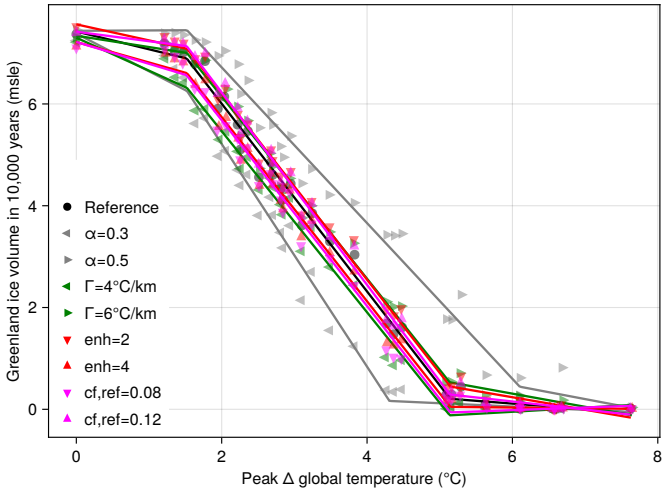

Extended Data Fig. 4 Linear fit of GrIS mass loss and peak global warming. Piecewise linear fits with two breakpoints for the relation between simulated Greenland ice volume in 10,000 years and peak global warning, separately for each set of model parameters.

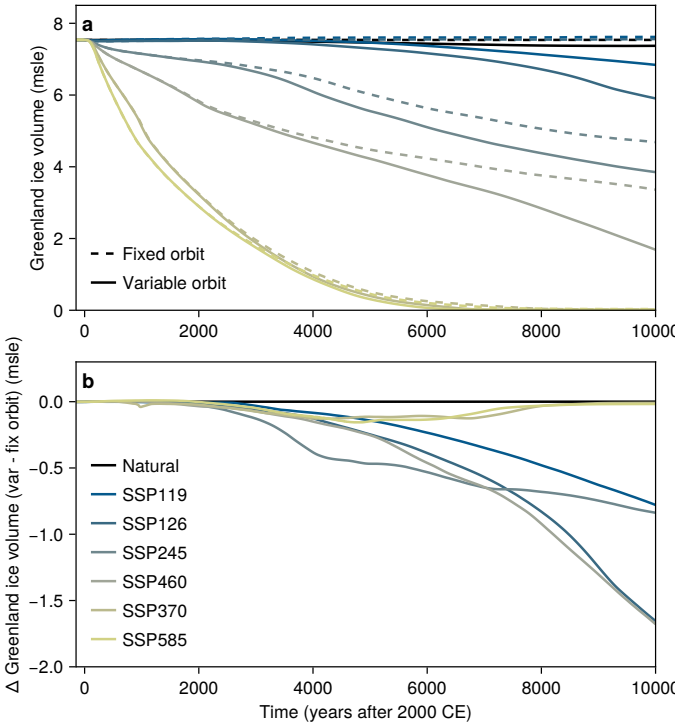

Extended Data Fig. 5 Effect of orbital forcing. (Top) Simulated GrIS volume for simulations with changing orbital parameters (solid) and fixed present-day orbital parameters (dashed). (Bottom) Differences in simulated GrIS volume due to varying orbital parameters.

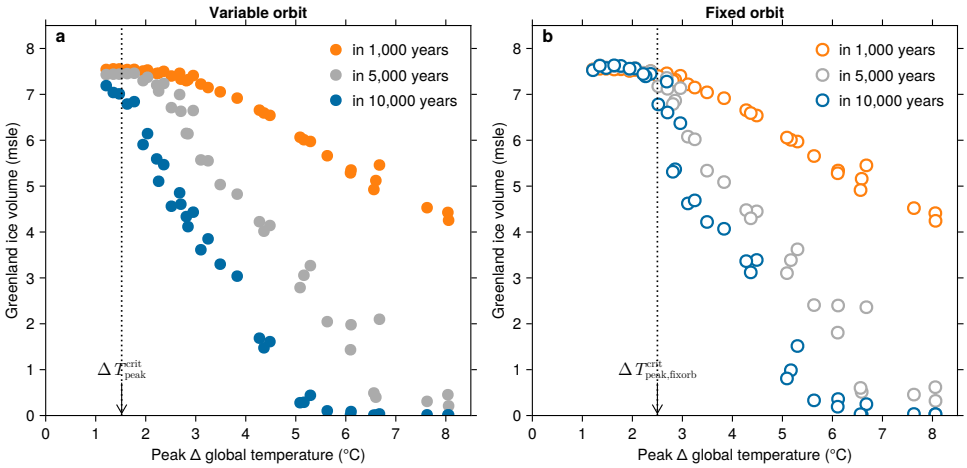

Extended Data Fig. 6 Variable vs fixed orbital parameters. **a** Simulated GrIS volume in metres of sea-level equivalent in 1,000, 5,000 and 10,000 years as a function of peak global warming relative to pre-industrial for all reference model simulations. **b** Same as **a** but for the simulations with prescribed present-day orbital parameters.

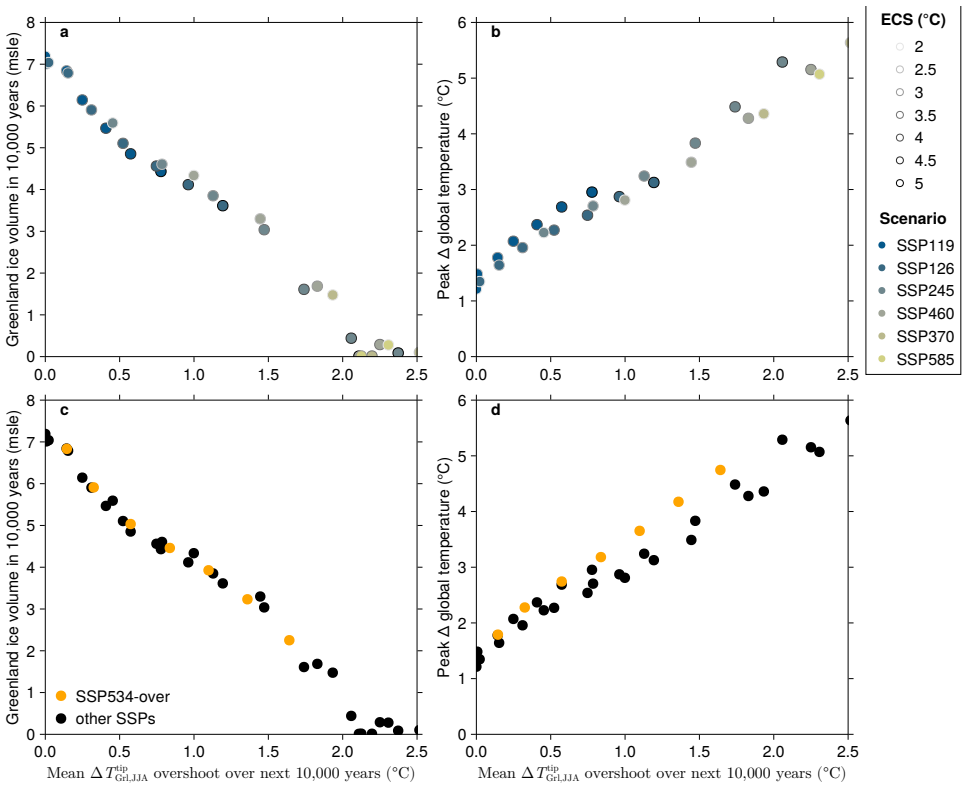

Extended Data Fig. 7 Relation of GrIS volume and temperature overshoots. **a** Simulated GrIS volume in 10,000 years as a function of the average temperature relative to the Greenland summer tipping point temperature ($\Delta T^{tip}_{Grl,JJA}$ ≈1.9°C) for all the simulations with different scenarios and ECS. **b** Peak global warming versus the average overshoot of the Greenland summer tipping point temperature. Panels **c,d** are similar to **a,b** but showing additionally results from model simulations for the overshoot scenario SSP534-over in orange, while all other scenarios are shown in black.

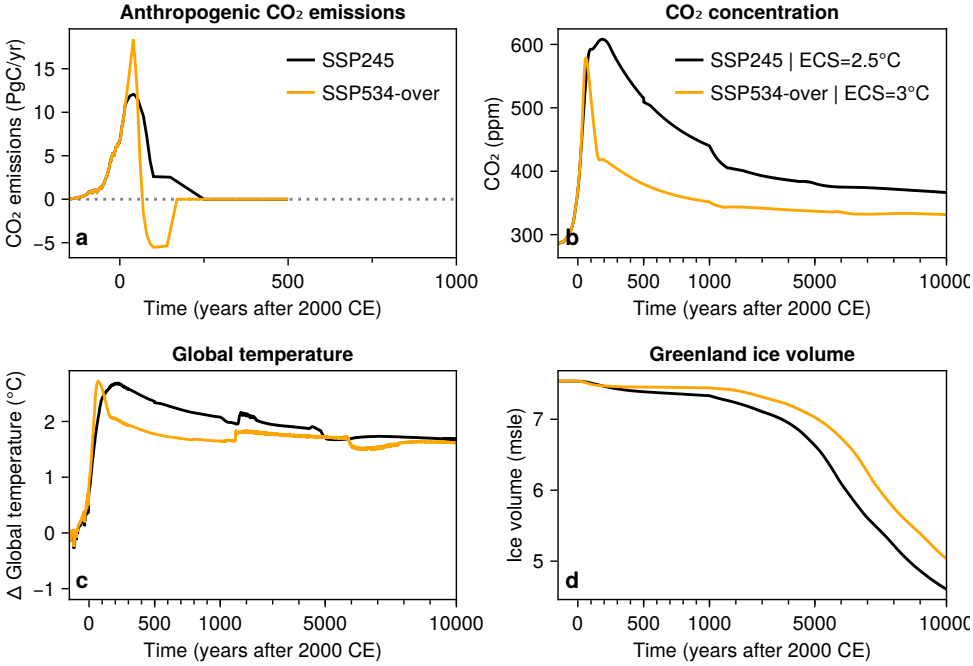

Extended Data Fig. 8 Impact of large negative carbon emissions. Comparison of two simulations with similar peak global warming but very different anthropogenic emission scenarios, SSP245 with an ECS of 2.5°C (black) and SSP534-over with an ECS of 3°C (orange).

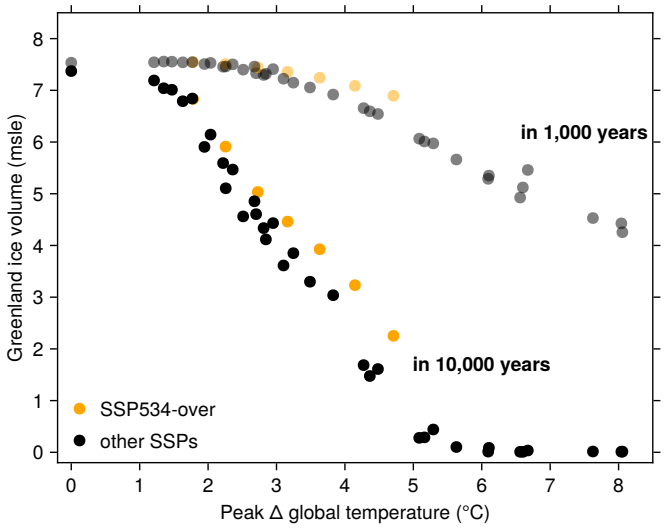

Extended Data Fig. 9 Relation between long-term GrIS mass loss and peak global warming for overshoot scenario. Relation between long-term (at 1000 and 10000 years into the future) Greenland ice loss and peak global warming for the overshoot scenario SSP534-over (orange) and the other considered SSP scenarios (black).